

# Dealkylation of Coenzyme B<sub>12</sub> and Related Organocobalamins: Ligand Structural Effects on Rates and Mechanisms of Hydrolysis

Michael P. Jensen and Jack Halpern\*

Contribution from the Department of Chemistry, University of Chicago, 5735 South Ellis Avenue, Chicago, Illinois 60637

Received July 6, 1998

**Abstract:** Rates and mechanisms of dealkylations of coenzyme B<sub>12</sub>, Ado-B<sub>12</sub>, and of five related organocobalamin compounds, including 2',5'-dideoxyadenosyl, 3',5'-dideoxyadenosyl, 2',3',5'-trideoxyadenosyl, 1,5-dideoxyribofuranosyl, and tetrahydrofurfuryl complexes (2'dAdo-B<sub>12</sub>, 3'dAdo-B<sub>12</sub>, 2',3'ddAdo-B<sub>12</sub>, 1dRF-B<sub>12</sub>, and THFF-B<sub>12</sub>, respectively), were determined in acidic solutions. In each case, competitive homolytic and acid-induced hydrolytic cobalt–carbon bond decomposition pathways were identified. Two mechanisms were observed for Co–C bond hydrolysis: the first, involving initial depurination followed by elimination from an organometallic intermediate, predominates for 2'dAdo-B<sub>12</sub> and 2',3'ddAdoB<sub>12</sub>; the second path, involving ring-opening protonation at the ribofuranosyl oxygen, analogous to hydrolyses of simple  $\beta$ -hydroxy and  $\beta$ -alkoxy complexes, predominates for the other four complexes. The rates of both hydrolysis pathways exhibited a marked dependence on the ligand functional groups. Ado-B<sub>12</sub>, the most substituted and most stable of the complexes, decomposes nearly 10 000-fold more slowly than the least stable, unsubstituted THFF-B<sub>12</sub> complex. Systematic variation of the hydroxy and adenine substituents on the furanosyl ring afforded insights into the roles of these substituents in effecting this large stabilization toward hydrolysis. Because of the extreme hydrolytic stability of the coenzyme, biologically relevant homolytic dissociation of 5'-deoxyadenosyl radical is competitive with hydrolysis over a wide pH range where the unprotonated, base-on form is kinetically dominant. Determination of the pH dependence of the dealkylation rates of Ado-B<sub>12</sub>, 2'dAdo-B<sub>12</sub>, and 3'dAdo-B<sub>12</sub> afforded quantification of the competition between homolytic and hydrolytic paths. In contrast to hydrolysis, the limiting homolytic Co–C bond dissociation rate was found to be insensitive to hydroxy substitution. Finally, broader issues relevant to organocobalamin chemistry and also bearing on earlier observations, are considered, among them protonation equilibria and dealkylation kinetics of organocobalamins, and fitting procedures for axial base dissociation equilibria.

## Introduction

Coenzyme B<sub>12</sub> (5'-deoxyadenosylcobalamin, abbreviated Ado-B<sub>12</sub>, Scheme 1) serves as a cofactor for a family of enzymatic reactions, a common feature of which is the 1,2-interchange of a hydrogen atom and an adjacent group (X = OH, NH<sub>2</sub>, etc.).<sup>1</sup> The generally accepted pathway of these reactions involves the minimal sequence of steps in Scheme 2, notably (a) enzyme-induced homolytic dissociation of the Co–C bond, (b) H-abstraction from the substrate by the 5'-deoxyadenosyl (Ado•) radical, (c) rearrangement of the resulting substrate radical, and (d) transfer of a hydrogen atom from 5'-deoxyadenosine to the resulting product radical to complete the rearrangement (e.g., of succinate to methylmalonate) and regenerate Ado•.<sup>2</sup>

The Co–C bond dissociation energy of free coenzyme B<sub>12</sub> has been estimated to be in the range of 26 to 31 kcal/mol.<sup>3–5</sup> Under enzymatic reaction conditions the rate of Co–C bond dissociation is enhanced by a factor up to 10<sup>10</sup> compared with that of the free coenzyme. This Co–C bond-weakening has been

attributed to steric effects associated with enzyme-induced conformational distortion of the corrin ring, although other interpretations are not precluded.

A striking feature of the organometallic chemistry of coenzyme B<sub>12</sub> is the minimization of nonproductive side reactions, for example  $\beta$ -hydride<sup>6</sup> or  $\beta$ -alkoxide<sup>7–14</sup> eliminations that would cleave the Co–C bond irreversibly (Scheme 3). The latter

(6) (a) Ng, F. T. T.; Rempel, G. L.; Mancuso, C.; Halpern, J. *Organometallics* **1990**, *9*, 2762. (b) Garr, C. D.; Finke, R. G. *J. Am. Chem. Soc.* **1992**, *114*, 10440. (c) Lott, W. B.; Chagovitz, A. M.; Grissom, C. B. *J. Am. Chem. Soc.* **1995**, *117*, 12194.

(7) (a) Barker, H. A.; Weissbach, H.; Smyth, R. D. *Proc. Natl. Acad. Sci. U.S.A.* **1958**, *44*, 1093. (b) Barker, H. A.; Smyth, R. D.; Weissbach, H.; Tooney, J. I.; Ladd, J. N.; Volcani, B. E. *J. Biol. Chem.* **1960**, *235*, 480. (c) Barker, H. A.; Smyth, R. D.; Weissbach, H.; Munch-Petersen, A.; Toohey, J. I.; Ladd, J. N.; Volcani, B. E.; Wilson, R. M. *J. Biol. Chem.* **1960**, *235*, 181. (d) Weissbach, H.; Ladd, J. N.; Volcani, B. E.; Smyth, R. D.; Barker, H. A. *J. Biol. Chem.* **1960**, *235*, 1462. (e) Ladd, J. N.; Hogenkamp, H. P. C.; Barker, H. A. *Biochem. Biophys. Res. Commun.* **1960**, *2*, 143. (f) Hogenkamp, H. P. C.; Barker, H. A. *J. Biol. Chem.* **1961**, *236*, 3097.

(8) Hogenkamp, H. P. C.; Oikawa, T. G. *J. Biol. Chem.* **1964**, *239*, 1911.

(9) (a) Hogenkamp, H. P. C., in ref 1; Vol. 1, Ch. 9, pp 312–4. (b) Johnson, A. W.; Shaw, N. *J. Chem. Soc. A* **1962**, 4608.

(10) (a) Gerards, L. E. H.; Balt, S. *Recl. Trav. Chim. Pays-Bas* **1992**, *111*, 411. (b) Gerards, L. E. H.; Balt, S. *Recl. Trav. Chim. Pays-Bas* **1994**, *113*, 137.

(11) Hogenkamp, H. P. C.; Rush, J. E.; Swenson, C. A. *J. Biol. Chem.* **1965**, *240*, 3641.

(12) Brown, K. L.; Salmon, L.; Kirby, J. A. *Organometallics* **1992**, *11*, 422.

(13) Schrauzer, G. N.; Sibert, J. W. *J. Am. Chem. Soc.* **1970**, *92*, 1022.

(1) Dolphin, D., Ed. *B<sub>12</sub>*; Wiley: New York, 1982.

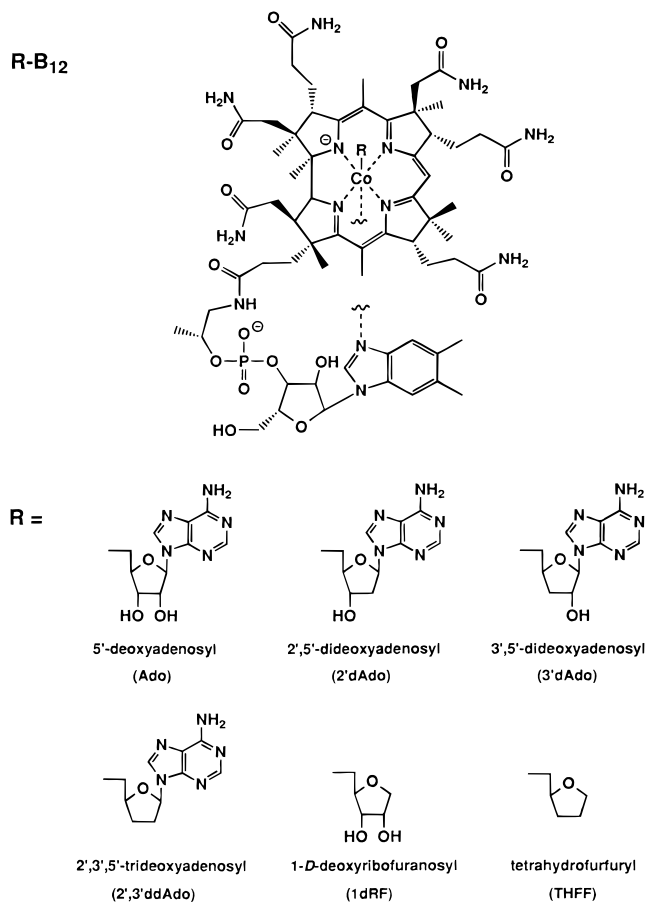
(2) Halpern, J. *Science* **1985**, *227*, 869.

(3) (a) Finke, R. G.; Hay, B. P. *Inorg. Chem.* **1984**, *23*, 3041. (b) Hay, B. P.; Finke, R. G. *J. Am. Chem. Soc.* **1986**, *108*, 4820. (c) Hay, B. P.; Finke, R. G. *Polyhedron* **1988**, *7*, 1469.

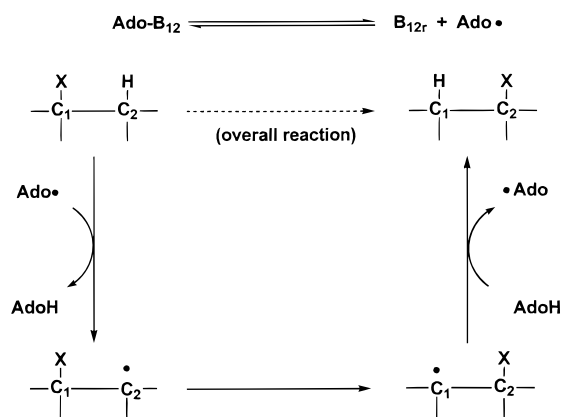
(4) Gerards, L. E. H.; Bulthuis, H.; de Bolster, M. W. G.; Balt, S. *Inorg. Chim. Acta* **1991**, *190*, 47.

(5) Halpern, J.; Kim, S.-H.; Leung, T. W. *J. Am. Chem. Soc.* **1984**, *106*, 8317.

## Scheme 1



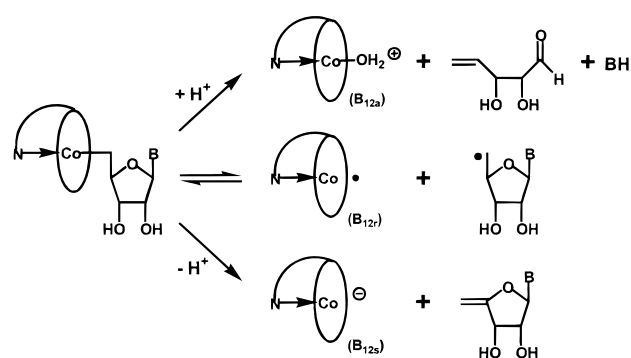
## Scheme 2



pathway was observed in early studies aimed at elucidation of the structure of Ado-B<sub>12</sub>, which indicated that cyanide was replaced on vitamin B<sub>12</sub> by a nucleoside that released 1 equiv. each of adenine and 2,3-dihydroxy-4-pentenal on acidic hydrolysis.<sup>7</sup> Such hydrolyses have since been widely observed for

(14) (a) Schrauzer, G. N.; Windgassen, R. *J. Am. Chem. Soc.* **1967**, *89*, 143. (b) Golding, B. T.; Holland, H. L.; Horn, U.; Sakrikar, S. *Angew. Chem., Int. Ed. Engl.* **1970**, *9*, 959. (c) Parfenov, E. A.; Chervyakova, T. G.; Edelev, M. G.; Kustanovich, I. M.; Yurkevich, A. M. *Zh. Obshch. Khim.* **1973**, *43*, 2777. (d) Silverman, R. B.; Dolphin, D.; Babior, B. M. *J. Am. Chem. Soc.* **1972**, *94*, 4028. (e) Silverman, R. B.; Dolphin, D. *J. Am. Chem. Soc.* **1973**, *95*, 1686. (f) Brown, K. L.; Ingraham, L. L. *J. Am. Chem. Soc.* **1974**, *96*, 7681. (g) Silverman, R. B.; Dolphin, D. *J. Am. Chem. Soc.* **1976**, *98*, 4626. (h) Espenson, J. H.; Wang, D. M. *Inorg. Chem.* **1979**, *18*, 2853. (i) Brown, K. L.; Ramamurthy, S. *Organometallics*, **1982**, *1*, 413. (j) Brown, K. L.; Ramamurthy, S.; Marynick, D. S. *J. Organomet. Chem.* **1985**, *287*, 377.

## Scheme 3



organocobalamins<sup>8–13</sup> and related organocobaloximes<sup>13,14</sup> with  $\beta$ -hydroxide or  $\beta$ -alkoxide substituents.

Heterolytic metal–alkyl bond hydrolysis, typically obeying the rate law,  $k_{\text{obs}} = k_0 + k_1[\text{H}^+]$ , has been observed for a wide range of complexes, including (H<sub>2</sub>O)<sub>5</sub>Cr<sup>III</sup>-R,<sup>15</sup> (protoporphyrin)-Fe<sup>III</sup>-R,<sup>16</sup> (tetrakis-sulfonatophthalocyanine)Co<sup>III</sup>-R,<sup>17</sup> (porphyrinato)Rh<sup>III</sup>-R,<sup>18</sup> (H<sub>2</sub>O)<sub>x</sub>Cu<sup>II</sup>-R,<sup>19</sup> and (H<sub>2</sub>O)<sub>x</sub>Hg<sup>II</sup>-R.<sup>20</sup> Available evidence suggests that Ado-B<sub>12</sub> is considerably more stable toward hydrolysis than many closely related organocobalt compounds. Previous studies in this laboratory demonstrated that tetrahydrofurfuryl cobalamin, THFF-B<sub>12</sub>, which lacks the hydroxide and adenine substituents of the 5'-deoxyadenosyl ligand, rapidly decomposes to aquo-cob(III)-alamin, B<sub>12a</sub> ( $t_{1/2} = 60$  min at pH 5, 25 °C).<sup>21</sup> The coenzyme is stable under these conditions and undergoes hydrolysis only under forcing conditions (e.g., boiling 0.1 N HCl).<sup>8</sup> Furthermore, 2'dAdo-B<sub>12</sub>, which differs from Ado-B<sub>12</sub> only by removal of a single ligand hydroxide (see Scheme 1), is much less stable than the coenzyme under such conditions.<sup>8</sup>

The research described in this paper was directed at exploring the origin and significance of this stabilization by elucidating the stoichiometry, kinetics, and mechanisms of Co–C bond disruption in modestly acidic solutions of a series of organocobalamins depicted in Scheme 1, in which the OH and adenine substituents of Ado-B<sub>12</sub> have been selectively replaced by hydrogen. The measurements revealed a ca. 10<sup>4</sup>-fold suppression of acid-catalyzed hydrolysis in going from THFF-B<sub>12</sub> to Ado-B<sub>12</sub> and provided some insights into the origin of this stabilization by OH and adenine substituents on the tetrahydrofurfuryl ring. (Note: Portions of this research have been previously reported.<sup>22</sup>) Related studies on selected cobaloxime compounds R-Co(DH)<sub>2</sub>(OH)<sub>2</sub> (R = Ado, 2'dAdo, THFF; DH<sub>2</sub> = dimethylglyoxime) are reported separately.<sup>23</sup>

(15) (a) Espenson, J. H. *Adv. Inorg. Bioinorg. Mech.* **1982**, *1*, 1. (b) Cohen, H.; Feldman, A.; Ish-Shalom, R.; Meyerstein, D. *J. Am. Chem. Soc.* **1991**, *113*, 5292.

(16) Sorek, Y.; Cohen, H.; Meyerstein, D. *J. Chem. Soc., Faraday Trans. 1* **1986**, *82*, 3431.

(17) Sorek, Y.; Cohen, H.; Meyerstein, D. *J. Chem. Soc., Faraday Trans. 1* **1989**, *85*, 1169.

(18) Wayland, B. B.; Van Voorhees, S. L.; Del Rossi, K. J. *J. Am. Chem. Soc.* **1987**, *109*, 6513.

(19) Cohen, H.; Meyerstein, D. *J. Chem. Soc., Faraday Trans. 1* **1988**, *84*, 4157.

(20) Halpern, J.; Tinker, H. B. *J. Am. Chem. Soc.* **1967**, *89*, 6427; and references therein.

(21) Kim, S.-H.; Chen, H. L.; Feilchenfeld, N.; Halpern, J. *J. Am. Chem. Soc.* **1988**, *110*, 3120.

(22) (a) Jensen, M. P.; Halpern, J. 206th National Meeting, American Chemical Society, Chicago, IL, August 22–27, 1993, Abstract INOR 310. (b) Jensen, M. P.; Zinkl, D. M.; Halpern, J. 209th National Meeting, American Chemical Society, Anaheim, CA, April 2–6, 1995, Abstract INOR 460.

(23) Jensen, M. P.; Zinkl, D. M.; Halpern, J. *Inorg. Chem.* **1999**, in press.

**Table 1.** <sup>1</sup>H NMR Spectra of Organocobalamins<sup>a</sup>

R-B <sub>12</sub>	pD	1'	2'	3'	4'	5' <sub>A</sub>	5' <sub>B</sub>	2,8	B2	B4	B7	R1	C10	C20H <sub>3</sub>	Pr3H <sub>3</sub>
Ado-	7.0	5.574 (d, 2.7)	4.553	3.768		0.582 (t, 9.8)	1.561 (d, 9.6)	8.014, 8.218	6.951	6.247	7.167	6.261 (d, 3.0)	5.943	0.484	1.220 (d, 6.3)
	1.6	5.559 (d, 2.1)		3.866		0.293 (t, 8.6)	1.406	8.159, 8.389	9.217	7.481	7.544	6.540 (d, 5.1)	6.959	0.769	1.170 (d, 6.3)
2'dAdo-	6.1	5.977 (dd, 3.7, 4.1)	2.291 <sup>b</sup>	3.891	2.291 <sup>b</sup>	0.525 (t, 8.9)	1.467 (d, 8.7)	8.035, 8.214	6.959	6.241	7.171	6.273 (d, 2.8)	5.958	0.463	1.229 (d, 6.3)
	1.6	5.937 (d, 6.6)		4.014		0.296 (t, 7.8)		8.180, 8.403	9.215	7.483	7.545	6.540 (d, 5.1)	6.956	0.756	1.166 (d, 5.1)
3'dAdo-	4.3	5.667 (s)	4.640	2.85 <sup>b</sup>	2.85 <sup>b</sup>	0.741 (t, 8.7)		7.975, 8.247	7.22	6.397	7.22	6.309 (br s)	6.100	0.469	1.22 (d)
	1.6	5.632 (s)				0.369 (t, 8.6)	1.263 (d, 7.5)	8.061, 8.414	9.219	7.489	7.548	6.543 (d, 5.1)	6.965	0.750	1.064 (d, 6.3)
2',3'ddAdo-	4.3	5.921 (dd, 3.0, 6.9)				1.499 (t, 7.1)	1.499 (d, 8.1)	8.068, 8.259	7.213	6.401	7.240	6.300 (d, 3.0)	6.113	0.431	1.209
	1dRF-	4.3		4.311 <sup>b</sup>	4.311 <sup>b</sup>	0.629 (t, 7.8)		N/A	7.173	6.374	7.223	6.310 (br s)	6.079	0.482	
THFF-	4.3					0.710 (t, 7.0); 0.665 (t, 7.1)	1.510 (d, 8.3)	N/A	7.026; 6.995	6.287; 6.272	7.199; 7.189	6.303	6.077; 6.016	0.521; 0.433	1.232 (d, 3.2); 1.212 (d, 3.2)

<sup>a</sup>  $\delta$  in ppm and  $J_{\text{HH}}$  in Hz. <sup>b</sup> Assignment ambiguous.

## Results and Discussion

The compounds in Scheme 1 were prepared by reactions of the corresponding tosyl esters with cob(D)alamin (vitamin B<sub>12</sub>s) and characterized by <sup>1</sup>H NMR spectroscopy (Table 1). Comparison with previously reported spectra of Ado-B<sub>12</sub><sup>24</sup> facilitated partial assignment of resonances and provided support for the assigned structures. Observation of the diastereotopic H5' methylene resonance near 0.5 ppm for all the compounds was consistent with the presence of Co–C5' bonds, and distinctive downfield H1' resonances confirmed the presence of intact glycosidic bonds in compounds containing such bonds.

**Protonation and Axial Base Equilibria.** Interpretation of the decomposition kinetics required a knowledge of the equilibria for protonation of the organocobalamins and for dissociation of the coordinated pendant 5,6-dimethyl benzimidazole ligand.<sup>25</sup>

In neutral aqueous solution organocobalamins exist as an equilibrium mixture of base-on and base-off forms ( $S_{\text{on}}$  and  $S_{\text{off}}$ , respectively, Scheme 4), whose concentrations are related by eq 1. Increasing acidity displaces this equilibrium by protonation

$$[S_{\text{on}}]/[S_{\text{off}}] = K_{\text{Co}} \quad (1)$$

of the pendant dimethylbenzimidazole ligand to form  $\text{SH}^+$  (Scheme 4), with an equilibrium constant defined by eq 2. The

$$[\text{H}^+][S_{\text{off}}]/[\text{SH}^+] = K_{\text{Bz}} \quad (2)$$

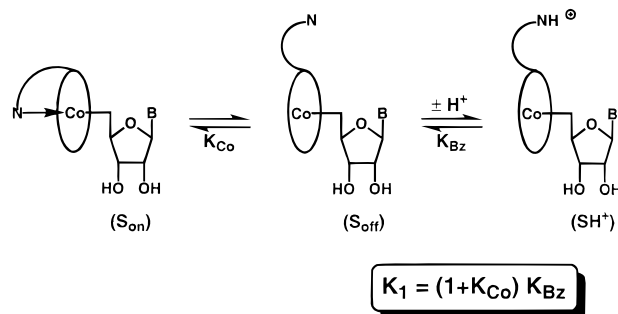
overall protonation equilibrium, thus, is described by eq 3.

$$K_1 = [\text{S}][\text{H}^+]/[\text{SH}^+] = ([S_{\text{on}}] + [S_{\text{off}}])[\text{H}^+]/[\text{SH}^+] = (1 + K_{\text{Co}})K_{\text{Bz}} \quad (3)$$

(24) (a) Summers, M. F.; Marzilli, L. G.; Bax, A. *J. Am. Chem. Soc.* **1986**, *108*, 4285. (b) Bax, A.; Marzilli, L. G.; Summers, M. F. *J. Am. Chem. Soc.* **1987**, *109*, 566. (c) Pagano, T. G.; Yohannes, P. G.; Hay, B. P.; Scott, J. R.; Finke, R. G.; Marzilli, L. G. *J. Am. Chem. Soc.* **1989**, *111*, 1484.

(25) (a) Ladd, J. N.; Hogenkamp, H. P. C.; Barker, H. A. *J. Biol. Chem.* **1961**, *236*, 2114. (b) Firth, R. A.; Hill, H. A. O.; Mann, B. E.; Pratt, J. M.; Thorp, R. G.; Williams, R. J. P. *J. Chem. Soc. A* **1968**, 2419. (c) Chemaly, S. M.; Pratt, J. M. *J. Chem. Soc., Dalton Trans.* **1980**, 2267.

## Scheme 4



While protonation is possible also at other sites (e.g.,  $\text{p}K = 3.5$  for adenosine<sup>26</sup> and 5.6 for  $\alpha$ -ribazole,<sup>27</sup> attenuated by coordination to cobalt in the coenzyme), <sup>1</sup>H NMR spectroscopic data are consistent with nearly exclusive protonation on the axial 5,6-dimethylbenzimidazole base. The methine (C10–H) resonance of Ado-B<sub>12</sub> is observed at 5.93 ppm at pD 7.0; the signal moves to 6.97 ppm in pD 2.1 solution, and to 7.06 ppm upon cleavage of the base.<sup>24</sup> The observed  $\Delta\delta$  (ppm), upon ca. 93% protonation, equals 92% of the difference between unprotonated Ado-B<sub>12</sub> and the base-removed complex. The benzimidazolium tautomer must comprise >98% of monoprotonated Ado-B<sub>12</sub>, and  $K_1$  corresponds approximately to the dissociation constant of this cation, as influenced by cobalt binding. Thus, in weakly acidic solution (i.e., where only monoprotonation is significant), the on–off equilibrium is described to good approximation by Scheme 4 and by eqs 1–3. While  $K_{\text{Bz}}$  might be expected to approximate  $K_a$  for the corrin-free  $\alpha$ -ribazole nucleotide, intramolecular hydrogen bonding causes some divergence.<sup>28</sup>

Room-temperature values of  $K_1$  for Ado-B<sub>12</sub>, 2'dAdo-B<sub>12</sub>, and 3'dAdo-B<sub>12</sub> were determined by titration, as described in the Experimental Section; details are provided in the Supporting Information (Section A, pp 2–6). Values at higher temperatures were extrapolated from measured temperature dependences of  $K_{\text{Co}}$  and  $K_{\text{Bz}}$  at fixed pH; details are provided in the Supporting

(26) Fasman, G. D., Ed. *Handbook of Biochemistry and Molecular Biology*, 3rd ed.; CRC Press: Cleveland, 1976; Vol. 1, p 158 and references therein.

(27) Brown, K. L.; Hakimi, J. M.; Nuss, D. M.; Montejano, Y. D.; Jacobsen, D. W. *Inorg. Chem.* **1984**, *23*, 1463.

(28) (a) Brown, K. L. *J. Am. Chem. Soc.* **1987**, *109*, 2277. (b) Brown, K. L.; Peck-Siler, S. *Inorg. Chem.* **1988**, *27*, 3548.

Information (Section B, pp 7–14). THFF-B<sub>12</sub>, 1dRF-B<sub>12</sub>, and 2',3'-ddAdo-B<sub>12</sub> were insufficiently stable to permit either direct titrations or equilibrium measurements; therefore,  $K_1$  values were deduced, as a last resort, from significantly different  $k'$  and  $k''$  limiting rates.

At higher acidities, further protonation at other basic sites may occur to form tautomeric mixtures of additional, multi-protonated species,  $\text{SH}_2^{2+}$ ,  $\text{SH}_3^{3+}$ ... $\text{SH}_n^{n+}$ , related by rapid proton-transfer equilibria through equilibrium constants  $K_2$ ,  $K_3$ ... $K_n$ , according to Scheme 5.

**Kinetics.** At constant pH (typical range 2–5), the kinetics of the overall decomposition reactions conformed to the first-order rate law of eq 4

$$-d[\text{S}]_{\text{tot}}/dt = k_{\text{obs}}[\text{S}]_{\text{tot}}, \quad \text{where}$$

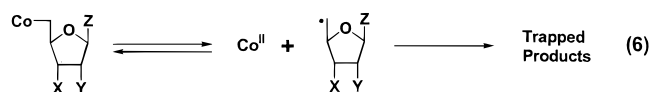
$$[\text{S}]_{\text{tot}} = [\text{S}] + [\text{SH}^+] + [\text{SH}_2^{2+}] + \dots + [\text{SH}_n^{n+}] \quad (4)$$

(where  $\text{S} = \text{R-B}_{12}$ ). The pH dependence of  $k_{\text{obs}}$  is described and interpreted in Scheme 5, according to which each of the species,  $\text{S}$ ,  $\text{SH}^+$ ,  $\text{SH}_2^{2+}$ , etc. undergoes decomposition with a characteristic rate constant,  $k_0$ ,  $k_1$ ,  $k_2$ , etc. Because multiple rapidly equilibrating isomers (e.g.,  $\text{S}_{\text{on}}$  and  $\text{S}_{\text{off}}$ , or tautomers of  $\text{SH}^+$ ) may contribute to a given term in the rate law and because rapid proton-transfer equilibria preclude kinetic distinction between decomposition of  $\text{SH}_i^{i+}$  and acid-catalyzed decomposition of  $\text{SH}_{(i-1)}^{(i-1)}$ ,  $1 < i < n$ , (e.g., between  $k_1[\text{SH}^+]$  and  $k'[\text{S}][\text{H}^+]$ ), Scheme 5 is generalized to include these alternative possibilities. Within the constraints of this study, i.e.,  $[\text{H}^+] \ll K_2$ , the observed rate law reduces, in accord with Scheme 5, to eq 5.

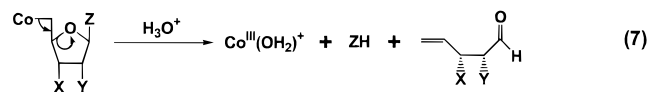
$$k_{\text{obs}} = \alpha(k_0 + k'[\text{H}^+]) + (1 - \alpha)k''[\text{H}^+] \quad (5)$$

**Decomposition Pathways.** For the range of conditions and compounds ( $\text{X}$ ,  $\text{Y} = \text{OH}$  or  $\text{H}$ ;  $\text{Z} = \text{adenine}$  or  $\text{H}$ ) encompassed by this study, three general decomposition pathways were identified, eqs 6–8.

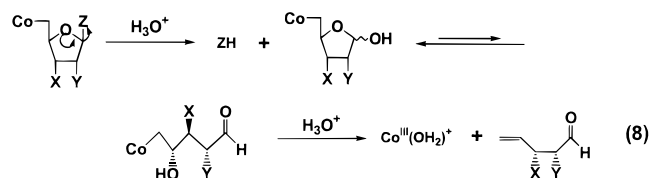
(i) Co–C homolysis



(ii) Co–C heterolysis induced by ring-opening protonation

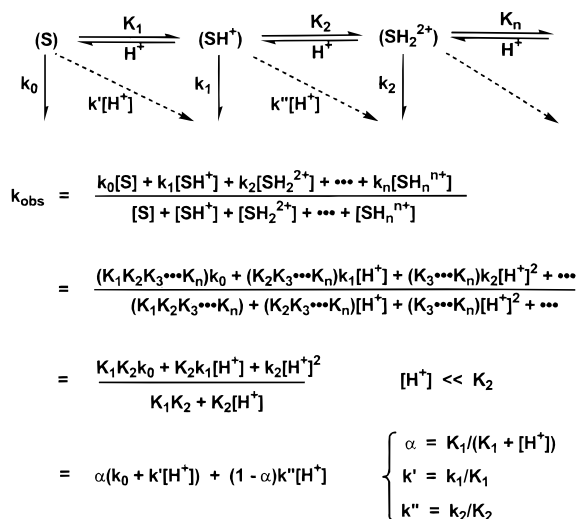


(iii) Co–C heterolysis induced by depurination



Departures, where noted, will be specifically addressed. Path (i) corresponds to the acid-independent term ( $k_0$ ) in the rate law (eq 5), while paths (ii) and (iii) are identified with the acid-dependent terms  $k'$  and  $k''$ . Paths (ii) and (iii) correspond to the same overall stoichiometry but involve different initial steps. Path (iii), which is applicable only when  $\text{Z} = \text{adenine}$ , is characterized by a potentially detectable organocobalt intermediate.

### Scheme 5



**Co–C Homolysis.** Homolytic Co–C bond dissociation produces initially cob(II)alamin ( $\text{B}_{12r}$ ) and an alkyl radical. Trapping of the resulting radical, either with an added trap or through spontaneous rearrangement or decomposition, inhibits  $\text{B}_{12r}$ -radical recombination so that the contribution of this path to the observed first-order rate constant of decomposition corresponds to the initial homolytic dissociation step.<sup>29</sup>

Two self-trapping routes that involve net hydrogen atom transfer are known for nucleosidyl radicals. 5'-Deoxyadenosyl radicals undergo internal substitution, accompanied by loss of a hydrogen atom, to form 5',8-anhydroadenosine (Scheme 6);<sup>30</sup> 5'-deoxyuridyl undergoes a different internal cyclization with net addition of a hydrogen atom.<sup>31</sup> In moderately acidic solutions an additional acid-promoted pathway also contributes to 5'-deoxyadenosyl decomposition and hence to trapping of the radical (Scheme 6). These pathways compete efficiently with  $\text{B}_{12r}$ -radical recombination so that limiting first-order kinetics ( $k_0$ ) for the homolytic decomposition pathway are observed when  $[\text{B}_{12r}] < 10^{-4} \text{ M}$ .<sup>3</sup>

Previous studies<sup>32</sup> have established that homolytic Co–C bond dissociation rates for base-on cobalamins are much higher than for the corresponding base-off species, hence the relationship between  $k_0$  and the base-on dissociation limit is given by eq 9. Measurements of  $k_{\text{homol}}$  and its temperature dependence

$$k_0 = k_{\text{homol}} K_{\text{Co}} / (1 + K_{\text{Co}}) \quad (9)$$

have previously been reported for Ado-B<sub>12</sub> under limiting trapping conditions in ethylene glycol,<sup>3a,c</sup> in mixed water/glycol,<sup>4</sup> and in aqueous pH 4.3 solution,<sup>5</sup> as well as in aqueous pH 7.0 solution without added radical trap.<sup>3b</sup>

**Co–C Heterolysis.** Acid-induced hydrolysis leading to heterolytic disruption of the Co–C bond proceeds by the two pathways depicted in eqs 7 and 8. The first involves ring-opening protonation of the ribofuranosyl oxygen, analogous to hydrolysis of simple  $\beta$ -hydroxy- and  $\beta$ -alkoxy-alkyl compounds,<sup>11,12</sup> and is typically cited as the dominant pathway for acid-promoted hydrolysis of Ado-B<sub>12</sub> and related nucleosidyl

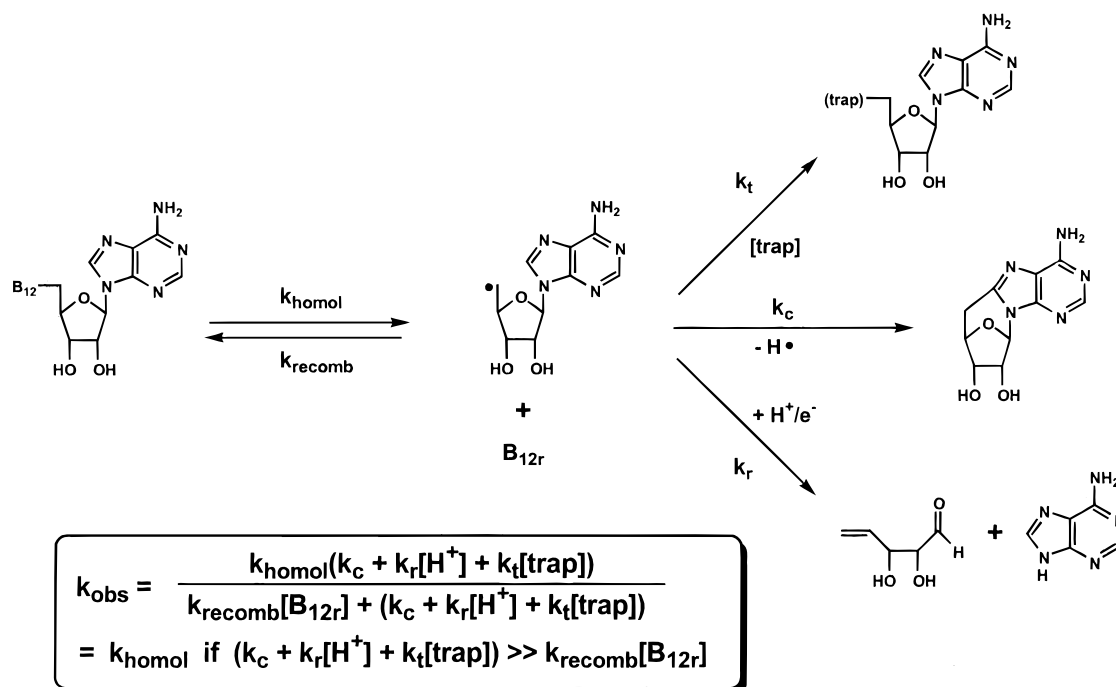
(29) Halpern, J. *Polyhedron* **1988**, 7, 1483.

(30) Hogenkamp, H. P. C. *J. Biol. Chem.* **1963**, 238, 477.

(31) Johnson, A. W.; Oldfield, D.; Rodrigo, R.; Shaw, N. *J. Chem. Soc.* **1964**, 4080.

(32) (a) Chemaly, S. M.; Pratt, J. M. *J. Chem. Soc., Dalton Trans.* **1980**, 2274. (b) Hay, B. P.; Finke, R. G. *J. Am. Chem. Soc.* **1987**, 109, 8012. (c) Schrauzer, G. N.; Grate, J. H. *J. Am. Chem. Soc.* **1981**, 103, 541. (d) Brown, K. L.; Brooks, H. B. *Inorg. Chem.* **1991**, 30, 3420.

## Scheme 6



cobalamins.<sup>8–10</sup> The second pathway involves initial loss of adenine, followed by hydrolysis of the resulting deoxyfuranosyl complex, both steps being acid-promoted. The extent of accumulation of the intermediate organocobalamin is determined by the relative rates of depurination and dealkylation. Since the final products of both pathways are identical, discrimination between them rests on kinetic considerations and, in favorable cases, on detection of the organocobalamin intermediate in the depurination pathway. The deconvolution of the overall rate law for such a sequence of pseudo-first-order processes into the component contributions and the evaluation of individual rate constants are straightforward.<sup>33</sup>

Acid-catalyzed depurination is a general reaction of purine nucleosides, of which Ado-B<sub>12</sub> and related cobalamins constitute a special subclass. It is anticipated that the rate of acid-catalyzed adenine loss from nucleosidyl cobalamins should be comparable to those of the corresponding nucleosides, since transmission of steric or electronic effects from cobalt to the C1'–N9 glycosidic bond is likely to be small. Ado-B<sub>12</sub> models lacking a 2'-OH should be especially susceptible to hydrolysis by this path.<sup>34</sup> Suppression of higher order paths (*k''*) is expected, because protonation of organocobalamin (*K*<sub>1</sub>) occurs predominantly at the dimethylbenzimidazole base and not on the purine.<sup>34f</sup>

Rates of acid-catalyzed hydrolysis of Ado-B<sub>12</sub> have been measured previously at high acidity (0.2–5.5 M HClO<sub>4</sub>, 0.1–9.5 M HCl, 0.7–9.8 M H<sub>2</sub>SO<sub>4</sub>) at temperatures from 16 to 40 °C,<sup>10</sup> in 1.0 N HCl at 27 °C,<sup>13</sup> and over the pH range 4–8 at 85 °C.<sup>3b</sup> While a minor uncatalyzed contribution was reported

for hydrolysis of the β-hydroxyethyl complex of a modified cobaloxime,<sup>14h</sup> the uncatalyzed hydrolyses of purine nucleosides are extremely slow (e.g., <10<sup>–8</sup> s<sup>–1</sup> at 80 °C for 2'-deoxyadenosine)<sup>34d</sup> and do not appear to have been observed experimentally.

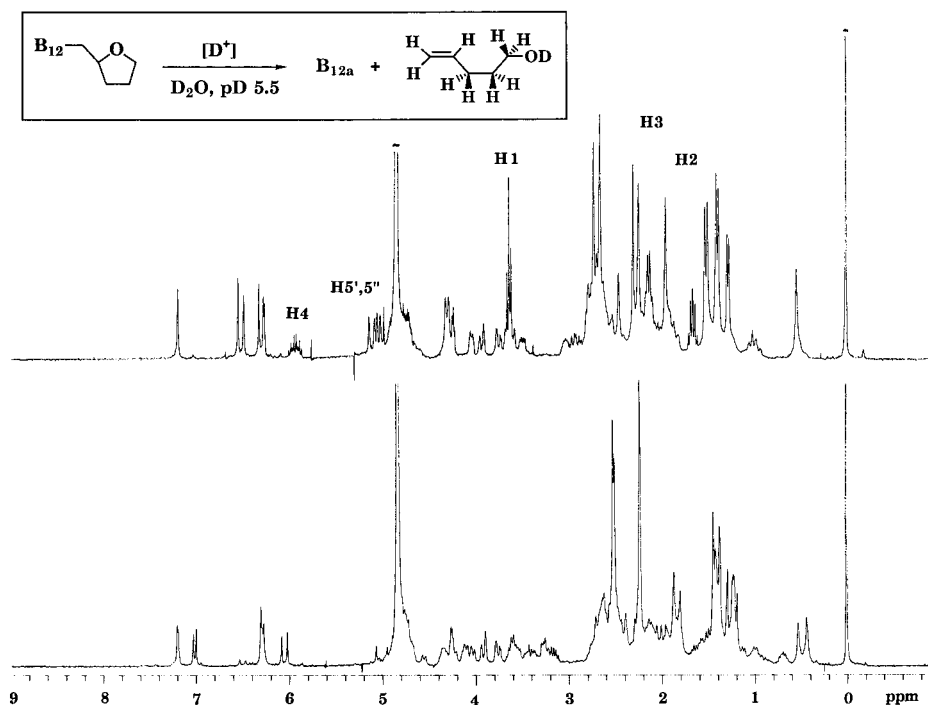
**Decomposition Studies. NMR Measurements and Organic Products.** Hydrolysis reactions in acidic D<sub>2</sub>O at room temperature were conveniently monitored by <sup>1</sup>H NMR spectroscopy, as illustrated for THFF-B<sub>12</sub> in Figure 1, and detailed for the other cobalamins in the Supporting Information (Section C, pp 15–23). Under these conditions, homolysis is negligible, <10<sup>–9</sup> s<sup>–1</sup> for Ado-B<sub>12</sub>.<sup>5</sup> The observations confirm the stoichiometry of eqs 7 and 8. Apart from some distinctive features that are noted below, this behavior extended to the other cobalamins, each of which decomposed to yield 1 equiv of B<sub>12a</sub>, olefin, and when appropriate, adenine (Table 2). Increasingly higher solution acidities and longer reaction times were necessary to force dealkylation of the complexes in the order THFF-B<sub>12</sub> < 1dRF-B<sub>12</sub> < 2',3'ddAdo-B<sub>12</sub> < 2'dAdo-B<sub>12</sub> < 3'dAdo-B<sub>12</sub> < Ado-B<sub>12</sub>.

THFF-B<sub>12</sub> was isolated as a nearly equimolar mixture of two C4 diastereomers with resolvable C10–H resonances at pD 4.3. Although the overall hydrolytic disappearance of organocobalamin and the corresponding appearance of B<sub>12a</sub> both followed approximate first-order kinetics, this was the result of the superposition of two rates differing by a factor of 4.1 (ΔΔG<sup>‡</sup> = 0.8 kcal/mol) for the two diastereomers, as shown in the Supporting Information (Section C, pp 16–17). Assignment of the two rates to specific isomers was not possible. This feature could not be detected by UV–visible monitoring of the kinetics since the two isomers are not spectroscopically distinguishable; composite rates determined by such a method are bound between those of either isomer, and differ from that of the relevant isomer by a factor of less than 4.1.

Hydrolyses of Ado-B<sub>12</sub> and 3'dAdo-B<sub>12</sub> at pD 1.6 produced transient minor resonances that could not be assigned to expected products, see Supporting Information (Section C, pp 19–20). Two signals appeared adjacent to the organocobalamin benz-

(33) Moore, J. W.; Pearson, R. G. *Kinetics and Mechanism*, 3rd ed.; Wiley: New York, 1981; pp 290–6.

(34) (a) Zoltewicz, J. A.; Clark, D. F.; Sharpless, T. W.; Grahe, G. J. *J. Am. Chem. Soc.* **1970**, *92*, 1741. (b) Hevesi, L.; Wolfson-Davidson, E.; Nagy, J. B.; Nagy, O. B.; Bruylants, A. *J. Am. Chem. Soc.* **1972**, *94*, 4715. (c) Panzica, R. P.; Rousseau, R. J.; Robins, R. K.; Townsend, L. B. *J. Am. Chem. Soc.* **1972**, *94*, 4708. (d) Garrett, E. R.; Mehta, P. J. *J. Am. Chem. Soc.* **1972**, *94*, 8532. (e) York, J. L. *J. Org. Chem.* **1981**, *46*, 2171. (f) Remaud, G.; Zhou, X.-X.; Chattopadhyaya, J.; Oivanen, M.; Lonnberg, H. *Tetrahedron* **1987**, *43*, 4453. (g) Oivanen, M.; Lonnberg, H.; Kazimierzczuk, Z.; Shugar, D. *Nucleosides Nucleotides* **1989**, *8*, 133. (h) Seela, F.; Mersmann, K. *Helv. Chim. Acta* **1992**, *75*, 1885.



**Figure 1.**  $^1\text{H}$  NMR spectra of THFF- $\text{B}_{12}$  in pD 5.5 solution (0.10 M  $d_3$ -acetate buffer) immediately after dissolution (bottom) and after standing for 24 h at room temperature (top). Peaks corresponding to product 4-pentenol are identified with labels.

imidazole signal, one just upfield of the B2–H peak at 9.20 ppm and the other between the B4–H and B7–H peaks at 7.51 ppm. Furthermore, the Ado- $\text{B}_{12}$  H1' signal split into overlapping doublets. These observations are consistent with the known hydrolysis of Ado- $\text{B}_{12}$  corrin amide side chains to carboxylate.<sup>35</sup> Evidence for hydrogen bonding between a specific side chain amide and the uncoordinated, unprotonated axial base was reported previously.<sup>28</sup> Hydrolysis of this side chain could disturb the axial base equilibrium by destabilizing the base-off, unprotonated form ( $S_{\text{off}}$ , Scheme 4) so that the resonances of the modified complex should appear offset slightly from those of parent complex. The alternative possibility that the signals result from axial nucleotide hydrolysis is unlikely, given the extreme stability of the  $\alpha$ -ribose nucleotidyl glycosidic bond.<sup>7b,34g</sup> Accumulation of the putative carboxylate complex is minor and does not appear to be competitive with the dealkylations of the other four complexes or with those of Ado- $\text{B}_{12}$  and 3'dAdo- $\text{B}_{12}$  at higher pH.

Transient  $^1\text{H}$  NMR peaks, slightly downfield of initial B2–H (9.25 vs 9.22 ppm) and C10–H (7.02 vs 6.96 ppm) signals, were observed during hydrolyses of 2',3'ddAdo- $\text{B}_{12}$  and 2'dAdo- $\text{B}_{12}$ , as shown in the Supporting Information (Section C, pp 21–23). Accompanying these, in the case of 2'dAdo- $\text{B}_{12}$ , were broad resonances at 0.20 and 0.50 ppm, on either side of the distinctive 5'-methylene signal. The organocobalamin resonances persisted even after the peaks of free adenine began to grow in. These observations indicate the formation of an intermediate mixture of anomeric (5-deoxyribofuranosyl) cobalamins resulting from depurination (i.e., hydrolysis of adenine) of the ribofuranosyl ligand, eq 8. This is consistent with the expectation noted earlier that glycosidic bonds of 2'-deoxyadenosyl complexes should be particularly prone to such hydrolysis. The intermediate B2–H and C10–H resonances are shifted slightly downfield to positions coincident with those reported for 5'-deoxyadenosyl

cobinamide lacking an axial base,<sup>30</sup> presumably due to elimination of adenine-protonated, base-on tautomers, and a pair of broad 5' methylene signals result from slow anomeric interconversion of the deoxyribofuranosyl ligand. Hydrolysis of 2',3'ddAdo- $\text{B}_{12}$  at pD 1.6 was monitored by  $^1\text{H}$  NMR spectroscopy, and the data were fit to consecutive depurination ( $1.5 \times 10^{-4} \text{ s}^{-1}$ ) and dealkylation ( $6.3 \times 10^{-4} \text{ s}^{-1}$ ) steps. This interpretation also is consistent with qualitative observations of the hydrolysis of 2'dAdo- $\text{B}_{12}$  at pD 1.6, but at the higher acidity (1.0 M DCl) required to monitor the reaction conveniently, the relative magnitudes of the depurination ( $7.0 \times 10^{-4} \text{ s}^{-1}$ ) and dealkylation ( $9.6 \times 10^{-5} \text{ s}^{-1}$ ) steps were reversed, and substantial generation of intermediate was observed, ca.  $(0.75)[2'd\text{Ado-B}_{12}]_0$ . Thus, it would appear that 2'dAdo- $\text{B}_{12}$  and 2',3'ddAdo- $\text{B}_{12}$  decompose predominantly through initial depurination. No evidence for this pathway was found for the other cobalamins.

**Decomposition Studies. Kinetics, Mechanisms, and Effects of Substituents.** Decomposition rates at 20 °C were monitored conveniently by UV–visible spectroscopy. Pseudo-first-order rate constants for each complex were determined over a range of pH, and the pH-dependence was fit to Scheme 5. The results are summarized in Table 3; observed and calculated rate–pH profiles are compared in Figure 2. Rate data and fits are presented in the Supporting Information (Section D, pp 24–30).

Several observations and conclusions are noteworthy. First, results for Ado- $\text{B}_{12}$  in the present study (i.e.,  $k'' \leq 2.9 \times 10^{-5} \text{ M}^{-1} \text{ s}^{-1}$  at 20 °C) are in reasonable agreement with previous measurements, which yielded  $k''$  values of  $7.4 \times 10^{-5} \text{ M}^{-1} \text{ s}^{-1}$  at 27 °C<sup>13</sup> and  $(0.85\text{--}2.7) \times 10^{-5} \text{ M}^{-1} \text{ s}^{-1}$  at 25 °C.<sup>10</sup> As anticipated, no significant contributions from  $k_0$ , i.e., from Co–C bond homolysis<sup>3,5</sup> or uncatalyzed hydrolysis, could be detected at 20 °C. Second, the observed rates and fitted values of  $k'$  and  $k''$  span an impressively large range, approaching 4 orders of magnitude. Ado- $\text{B}_{12}$  clearly is the most stable of the cobalamins that were studied, and all three ribofuranosyl substituents,

(35) (a) Morley, C. G. D.; Blakley, R. L.; Hogenkamp, H. P. C. *Biochemistry* **1968**, *7*, 1231. (b) Anton, D. L.; Hogenkamp, H. P. C.; Walker, T. E.; Matwiyoff, N. A. *J. Am. Chem. Soc.* **1980**, *102*, 2215.

Table 2. <sup>1</sup>H NMR Spectra of Products and Yields for Organocobalamin Hydrolysis

Cobalamin	Reaction Conditions	Yields, %		Sugar Structure	<sup>1</sup> H NMR Spectra of Sugars, δ and J <sub>HH</sub>						
		B <sub>12a</sub>	Adenine		1	2	3	4	5 <sub>A</sub>	5 <sub>B</sub>	
	pD 5.5 < 24 hr	87	--	92		3.63 (6.8)	1.65 (7.5)	2.13 (7.0)	5.92 (17.1, 10.2)	5.10 (2.0)	5.02 (D <sub>2</sub> O)
	pD 4.3 70 hr	98	--	83		3.65 (6.6)	1.66 (7.2)	2.14 (6.6)	5.82 (17.1, 10.8)	5.04 (1.5)	4.97 (CDCl <sub>3</sub> )
	pD 4.3 13 days	114	95	89		9.76	2.37 (5.9)	2.52 (6.5)	5.81 (17.0, 10.4)	5.04 (1.5)	5.00 (CDCl <sub>3</sub> )
	1.0 M DCI 7.0 hr	102	64	94		9.83 (1.3, 1.0)	2.68 2.70 (dd ?)	4.66 (6.5)	5.89 (17.1, 10.4)	5.31 (1.2)	5.17 (CDCl <sub>3</sub> )
	0.05 M DCI > 35 days	86	60	60		9.58 (8.0)	6.17 (15.3)	7.09 (11.0)	6.59 (17.1, 9.5)	5.74	5.62 (CDCl <sub>3</sub> )
	0.05 M DCI > 69 days	118	70	89		9.62			5.89 (7.1) (17.3, 10.0)	5.18	5.14 (D <sub>2</sub> O)
	0.05 M DCI > 69 days	118	70	89		9.73	3.55 (5.4)		5.96 (7.1) (17.3, 10.3)	5.36	5.32 (D <sub>2</sub> O)

namely 2'-OH, 3'-OH, and adenine, contribute to conferring stability toward hydrolysis. Removal of any of these enhances markedly the decomposition rate of the resulting complex. Possible origins of these stabilization effects are considered later.

As noted earlier, eqs 7 and 8, hydrolytic dealkylation of nucleosidyl cobalamins can proceed through two pathways, as exemplified by the kinetic plots for Ado-B<sub>12</sub> and 2'dAdo-B<sub>12</sub> in Figure 3; whereas Ado-B<sub>12</sub> decomposes with clean first-order kinetics, the decomposition of 2'dAdo-B<sub>12</sub> exhibits biphasic kinetics, the slower initial step being attributable to depurination and the terminal first-order step to hydrolysis of the depurinated cobalamin. As anticipated, the *k'* values for depurinations of 2'dAdo-B<sub>12</sub> and 2',3'ddAdo-B<sub>12</sub>, derived from such kinetic plots, agree with literature data<sup>34</sup> for hydrolysis of the corresponding nucleosides (Table 4). For both the cobalamins and nucleosides, OH substituents on the 2' and 3' positions inhibit cleavage of the glycoside bond, 2'dAdo-B<sub>12</sub> being more stable than 2',3'ddAdo-B<sub>12</sub>, and adenine loss from 3'dAdo-B<sub>12</sub> and Ado-B<sub>12</sub> being even slower. A 3'-OH substituent suppresses the rate of glycosidic bond rupture by a factor of ca. 10<sup>2</sup>, while suppression by a 2'-OH substituent exceeds a factor of 10<sup>3</sup>.


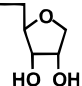
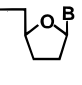
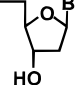
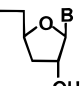
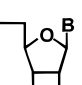
Since neither THFF-B<sub>12</sub> nor IdRF-B<sub>12</sub> possesses an adenine substituent, the slower rate of acid-induced hydrolysis of the latter demonstrates that OH substituents also suppress the direct ring-opening pathway. The rate effect is smaller, ca. 2–40-fold, than that on glycosidic bond rupture, but it is still significant. Presumably this also is relevant to the stabilization of 3'dAdo-B<sub>12</sub> and Ado-B<sub>12</sub> against acid-induced decomposition.

Stabilization by the adenine substituent is particularly marked, as reflected in the difference of ca. 10<sup>3</sup> between the *k''* values for IdRF-B<sub>12</sub> and Ado-B<sub>12</sub>. While this might be expected in view of the location of the base on the ring carbon adjacent to the active protonation site, the origin of the stabilization is unclear. Possible contributions are anomeric effects on basicity of the ring oxygen, steric and entropic effects on ring configurations, and competitive protonation of adenine.

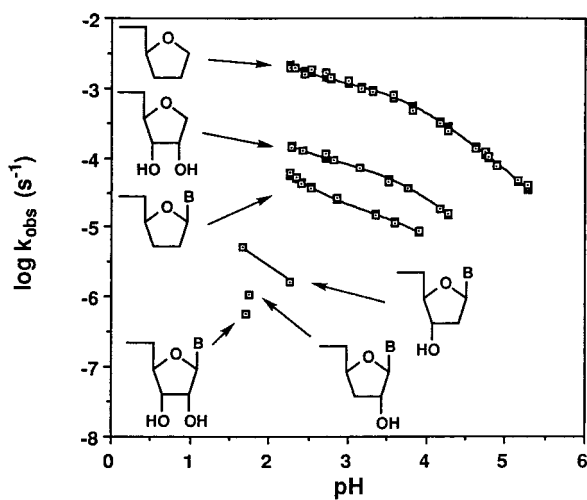
Of related interest are the dealkylations of the ribofuranosyl intermediates formed by depurinations of 2'dAdo-B<sub>12</sub> and 2',3'ddAdo-B<sub>12</sub>. The latter is nearly 100 times less stable, and has a *k''* value only ca. 5-fold lower than that of THFF-B<sub>12</sub>. The significantly larger stabilization effect of the 3-OH substituent, compared with that of the 2-OH, may imply that Co–C bond cleavage occurs from straight-chain aldehyde forms of the intermediate ligands.

Finally, axial base protonation influences both hydrolysis mechanisms. Observed *k'/k''* ratios are ca. 5–15 for depurination reactions and ca. 25–40 for dealkylations. Possible contributing factors are the increased positive charge and changes in corrin conformation associated with the base-on/base-off interconversion. These are difficult to quantify, a further complication being that the contributions of the base-on and unprotonated base-off complexes to the composite *k'* rate constant cannot be distinguished experimentally. However, corrin configuration effects should be small in glycosidic bond cleavage; therefore, the observation of significant *k'/k''* differences for the depurination reactions may imply that basicity of the axial benzimidazole

**Table 3.** Kinetic Parameters for Organocobalamin Dealkylation at 20.0 °C

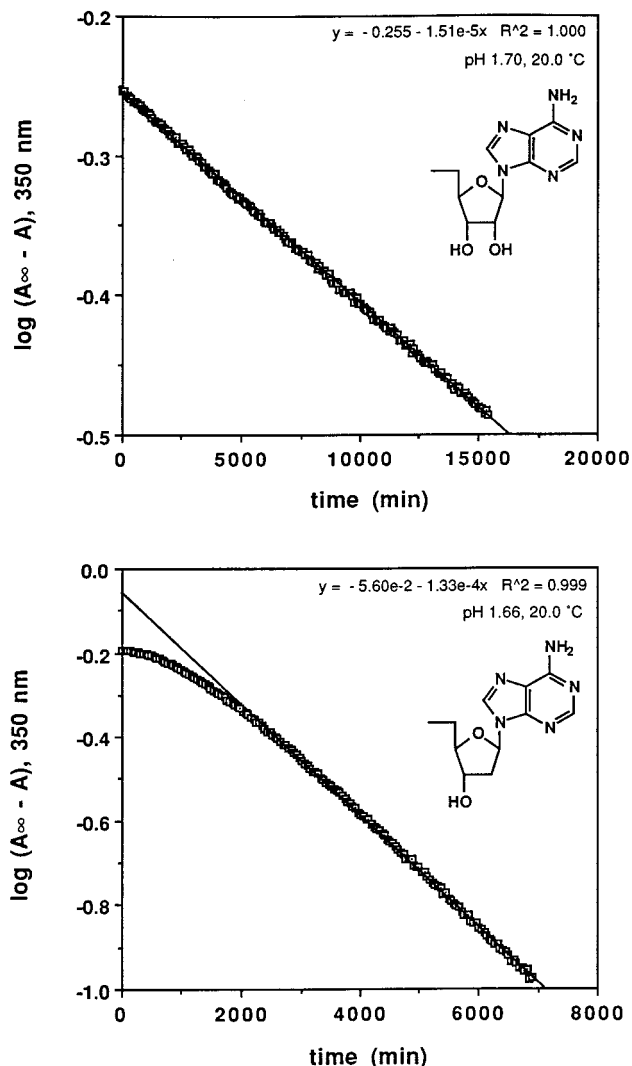
L	$k'$ ( $M^{-1}s^{-1}$ )	$k''$ ( $M^{-1}s^{-1}$ )	$pK_1$
	6.7	$1.8 \times 10^{-1}$	3.75
	$3.5 \times 10^{-1}$	$1.3 \times 10^{-2}$	3.6
	$1.3 \times 10^{-1}$ <sup>(a)</sup> fast	$7.7 \times 10^{-3}$ <sup>(a)</sup> $3.3 \times 10^{-2}$	3.9
	$1.1 \times 10^{-3}$ <sup>(a)</sup> $1.1 \times 10^{-2}$	$2.1 \times 10^{-4}$ <sup>(a)</sup> $3.8 \times 10^{-4}$	3.09
	slow	$\leq 5.8 \times 10^{-5}$	3.18
	slow	$\leq 2.9 \times 10^{-5}$	3.24

(a) Depurination step

**Figure 2.** Comparison of observed and calculated rates for acid-catalyzed hydrolyses of organocobalamin complexes at 20.0 °C.

does afford “kinetic buffer” protection in the pH region near  $pK_1$ .<sup>34f</sup>

**High-Temperature Measurements.** The high stabilities of Ado-B<sub>12</sub>, 3'dAdo-B<sub>12</sub>, and 2'dAdo-B<sub>12</sub> frustrated attempts to determine hydrolysis rates for the biologically relevant unprotonated forms (i.e.,  $k'$ ) at 20 °C. Therefore, measurements at higher pH, where the complexes are predominantly in unprotonated, base-on forms, were made at 90.0 °C where the dealkylation reactions proceed at convenient rates. Under these conditions, contributions from the homolytic Co–C decomposition were significant, and deconvolution required estimates of  $K_{Co}$  and  $K_1$  values at 90.0 °C. These were extrapolated from the temperature dependences of axial base equilibria recorded near the middle (pH = 4.3) and at the acid-independent limit (pH > 7) of the kinetic range. The equilibrium thermodynamic parameters, and derived  $pK_1$  estimates at 20.0 °C and at 90.0 °C, are summarized and compared with available literature data

**Figure 3.** First-order rate plots for hydrolyses of Ado-B<sub>12</sub> (top) and 2'dAdo-B<sub>12</sub> (bottom), as observed by UV–vis spectroscopy at 20.0 °C.

in Table 5. Fits are shown in the Supporting Information (Section B, pp 7–14).

Since the minor ligand variations involved are not expected to give rise to significant steric or electronic differences at cobalt, Ado-B<sub>12</sub>, 2'dAdo-B<sub>12</sub>, and 3'dAdo-B<sub>12</sub> should display similar axial base equilibria. Nevertheless, available data, including those from this study, reveal considerable variations in the relevant thermodynamic parameters (Table 5).<sup>3b,5,36</sup> Thus, reported  $\Delta H^\circ$  values range from 4.4 to 7.2 kcal/mol at neutral pH and from 2.0 to 4.5 kcal/mol at pH  $4.30 \pm 0.02$ , while  $\Delta S^\circ$  values range from 10 to 18 and from 5 to 12 cal/moleK, respectively. Inspection of the data reveals that the  $\Delta H^\circ$  and  $\Delta S^\circ$  variations are correlated within the two pH regions, so that  $\Delta\Delta H^\circ = T\Delta\Delta S^\circ$  (Figure 4). Linear fits to plots of both data sets yield a median temperature of 350 K, i.e., close to the temperature range (278–338 K) of the measurements. The variation in  $\Delta G^\circ$  among the measurements is small, suggesting that variations in  $\Delta H^\circ$  and  $\Delta S^\circ$  probably are artifactual compensations, reflecting modest discrepancies in estimates of base-on absorption limits. A similar situation could exist even in measurements made by NMR spectroscopy, because the slow experimental time scale merges the base-on and base-off signals and the base-on limit is never observed directly. This suggests

(36) Chen, H.; Yan, H.; Tang, W. *J. Inorg. Biochem.* **1993**, *52*, 109.



**Table 4.** Comparison of Organocobalamin and Nucleoside Hydrolysis Rates

5'-X	R	T (°C)	k' (M <sup>-1</sup> s <sup>-1</sup> )
B <sub>12</sub> <sup>-</sup>		20.0	1.3 × 10 <sup>-1</sup>
HO- <sup>34h</sup>		25	7.2 × 10 <sup>-2</sup>
B <sub>12</sub> <sup>-</sup>		20.0	1.1 × 10 <sup>-3</sup>
HO- <sup>34d</sup>		20	1.3 × 10 <sup>-3</sup>
B <sub>12</sub> <sup>-</sup>		20.0	2.9 × 10 <sup>-5</sup> (k'')
HO- <sup>34b</sup>		20	3 × 10 <sup>-6</sup>

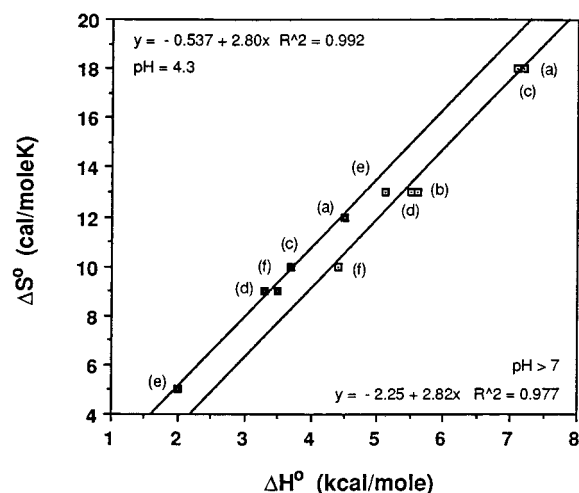
**Table 5.** Comparison of Axial Base Equilibrium Parameters

R-B <sub>12</sub>	pH	ΔH <sup>0</sup> (kcal/mole)	ΔS <sup>0</sup> (eu)	% off (20°C/90°C)	pK <sub>1</sub> (20°C/90°C)
	7.20	4.4	10	8.3/27.9	3.5/3.7
	4.28	3.3	9	20.5/43.5	
	6.9	7.1	18	4/31	3.6/3.8 <sup>ref. 36</sup>
	4.3	3.7	10	21/48	
	7.23	5.1	13	7.4/30.3	3.8/3.7
	4.31	2.0	5	27.6/42.9	
	7.23	5.5	13	6.1/28.3	3.4/3.5
	4.31	3.5	9	16.5/38.3	
	7.0	5.6	13	4/23 <sup>ref. 3</sup>	3.5/3.8 <sup>ref. 5</sup>
	7.6	7.2	18	3/28	
	4.3	4.5	12	16/45	

that apparent differences between axial base equilibrium parameters should be interpreted with caution.

Observed and calculated rates for anaerobic dealkylations of 2'dAdo-B<sub>12</sub>, 3'dAdo-B<sub>12</sub>, and Ado-B<sub>12</sub> at 90.0 °C over a ca. pH 3.3–6.1 range are summarized in Table 6 and Figure 5; rate data and fits are provided in the Supporting Information (Section E, pp 31–35). The pH-dependent rate data are broken down into acid-catalyzed ( $\alpha k'[\text{H}^+]$ ) and acid-independent ( $\alpha k_0$ ) contributions, and the resulting fits are compared in Figure 6. Because of reliance on radical self-trapping, observed  $k_0$  values should be taken as lower limits. Indeed, some slowing from initial rates was observed for Ado-B<sub>12</sub> and 3'dAdo-B<sub>12</sub> at the upper end of the covered pH range, and these data were omitted from the fitting procedure.

Several observations warrant comment. First, the rates for the different complexes converge with increasing pH toward a common lower limit corresponding to the homolysis rate constant,  $k_0 = (4.9 \pm 0.6) \times 10^{-5} \text{ s}^{-1}$ . Susceptibility to acid-induced hydrolytic decomposition follows the same trend as at

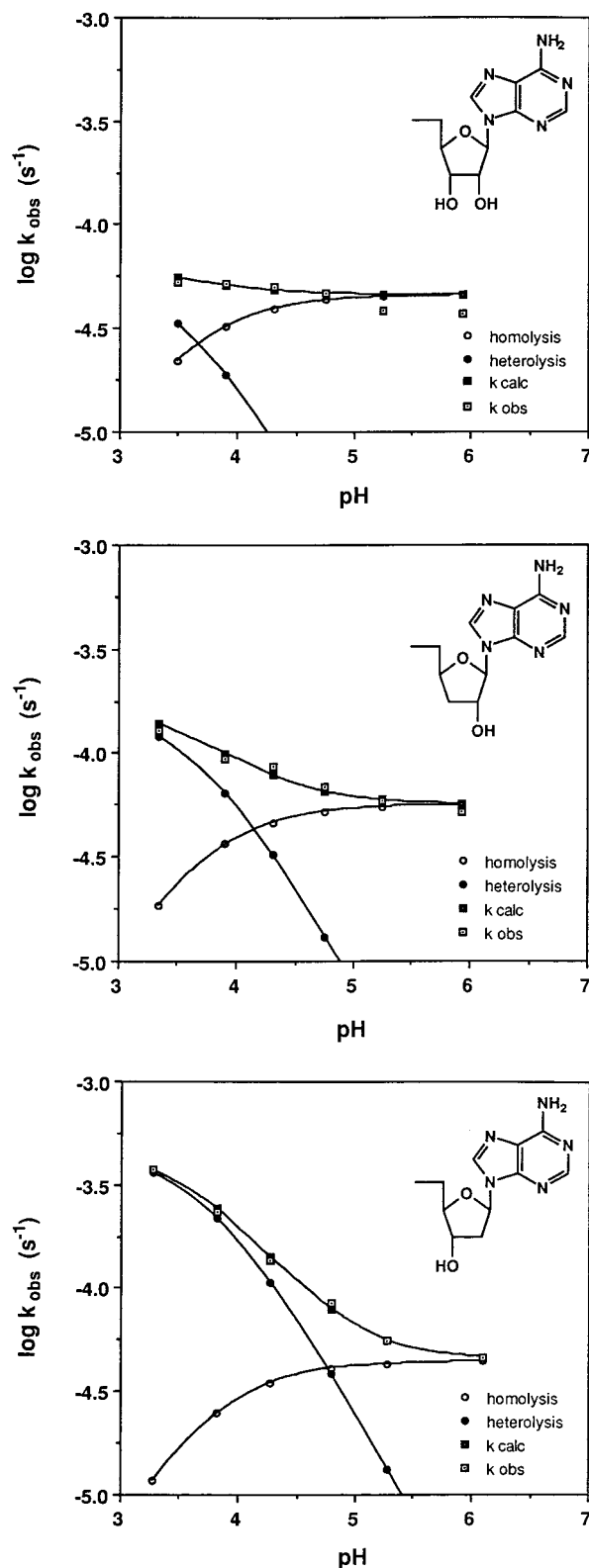
**Figure 4.** Comparison of axial base thermodynamic data for Ado-B<sub>12</sub>, 2'dAdo-B<sub>12</sub>, and 3'dAdo-B<sub>12</sub> in neutral solution and at pH 4.3 (■): a = Ado-B<sub>12</sub>,<sup>5</sup> b = Ado-B<sub>12</sub>,<sup>3b</sup> c = 2'dAdo-B<sub>12</sub>,<sup>36</sup> d = Ado-B<sub>12</sub>, this work; e = 3'dAdo-B<sub>12</sub>, this work; f = 2'dAdo-B<sub>12</sub>, this work.**Table 6.** Summary of Kinetic Parameters for Dealkylation at 90.0 °C

R-B <sub>12</sub>	k' (M <sup>-1</sup> s <sup>-1</sup> )	k <sub>0</sub> /k <sub>homol</sub> (s <sup>-1</sup> )	pK <sub>1</sub>
	2.6	4.4 × 10 <sup>-5</sup> 6.2 × 10 <sup>-5</sup>	3.7
	0.80	5.6 × 10 <sup>-5</sup> 8.1 × 10 <sup>-5</sup>	3.7
	0.21	4.6 × 10 <sup>-5</sup> 6.4 × 10 <sup>-5</sup>	3.5
	slow	4.8 × 10 <sup>-5</sup> 6.7 × 10 <sup>-5</sup>	3.8 <sup>5</sup>
	0.92	1.2 × 10 <sup>-5</sup> 1.5 × 10 <sup>-5</sup>	4.5 <sup>3b</sup>

(Deduced from Figure 5, 85°C)

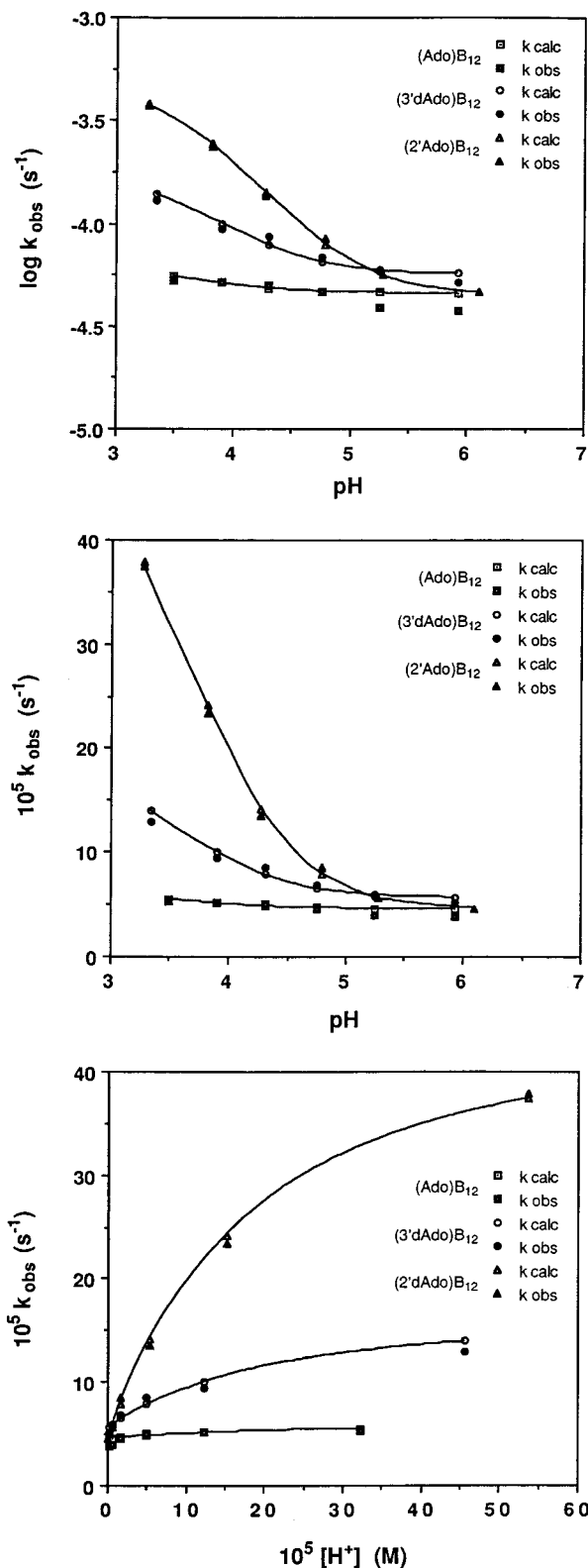
20 °C, i.e., Ado-B<sub>12</sub> < 3'dAdo-B<sub>12</sub> < 2'dAdo-B<sub>12</sub>. The ca. 12-fold span of relative heterolysis rates is nearly identical in magnitude to that for  $k''$  at 20 °C. In contrast, the  $k_0$  values show little variation and yield a common value for the base-on rate constant,  $k_{\text{homol}} = (6.9 \pm 1.0) \times 10^{-5} \text{ s}^{-1}$  at 90.0 °C in good agreement with the value of  $6.7 \times 10^{-5} \text{ s}^{-1}$  reported previously for Ado-B<sub>12</sub> from measurements at pH 4.3 under rigorous trapping conditions.<sup>5</sup>

The present results for Ado-B<sub>12</sub> are in quantitative disagreement (Table 6) with those of a related earlier study that reported thermolysis products and kinetics under similar conditions (pH 4.0–8.0, 85–110 °C) and estimated the hydrolytic component of the overall dealkylation from the pH-dependent fractional adenine yield.<sup>3b</sup> The limiting monocation decomposition rate (i.e.,  $k_1$  in Scheme 5) estimated from reported data (i.e., Figure 5 and Table 1 in ref 3b) was similar to the value obtained here (ca.  $2.9 \times 10^{-5} \text{ s}^{-1}$  at 85 °C versus  $6.3 \times 10^{-5} \text{ s}^{-1}$  at 90.0 °C). However, pK<sub>1</sub> was much higher, ca. 4.5,  $k_0$  was much smaller, and a minor hydrolytic contribution to  $k_0$  (<10%) was suggested on the basis of trace adenine production above pH 7. In the absence of a demonstration of complete Ado• radical trapping, of the detailed pH-rate profile and of independent estimation



**Figure 5.** Plots of pH dependences for observed and calculated dealkylation rates at 90.0 °C for Ado-B<sub>12</sub> (top), 3'dAdo-B<sub>12</sub> (middle), and 2'dAdo-B<sub>12</sub> (bottom). Homolytic ( $\alpha k_0$ ) and hydrolytic ( $\alpha k'[\text{H}^+]$ ) contributions to calculated rates are also shown.

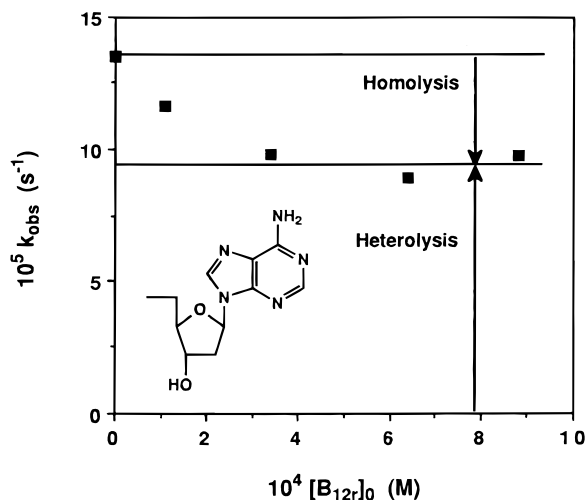
of the rate of homolysis from B<sub>12r</sub> inhibition, the results of the earlier study cannot be adequately assessed or compared with those of the present study. The proposed contribution from hydrolysis in the earlier work (77% at 85 °C and pH 4.3) is much larger than that deduced from the present study (ca. 18% at 90 °C and pH 4.3, presumably an upper limit since limiting



**Figure 6.** Comparison of effects of solution acidity on observed and calculated dealkylation rates at 90.0 °C for Ado-B<sub>12</sub>, 3'dAdo-B<sub>12</sub>, and 2'dAdo-B<sub>12</sub>. Data are shown as log(pH vs log  $k_{\text{obs}}$ , top), semilog(pH vs  $k_{\text{obs}}$ ), and normal ( $[\text{H}^+]$  vs  $k_{\text{obs}}$ , bottom) plots.

suppression of Ado•-B<sub>12r</sub> recombination by radical trapping was not demonstrated).

Recognizing the potential for uncertainty in fitting multiple parameters to the pH-dependent rate data, we performed a rigorous test of the 2'dAdo-B<sub>12</sub> fit: rates were measured as before at pH 4.3, but varying amounts of B<sub>12r</sub> were added to



**Figure 7.** Observed rates of dealkylation of 2'dAdo-B<sub>12</sub> plotted against initial B<sub>12r</sub> loadings at pH 4.28, 90.0 °C.

promote 2'dAdo•-B<sub>12r</sub> radical recombination and suppress homolysis. Observed rates decreased asymptotically with increasing B<sub>12r</sub> loadings, see Supporting Information (Section F, pp 36–38), toward a limiting value of  $9.4 \times 10^{-5} \text{ s}^{-1}$  (Figure 7), within experimental error of the fitted  $\alpha k'[\text{H}^+]$  value of  $1.06 \times 10^{-4} \text{ s}^{-1}$ . Further support is provided by good agreement between the fitted parameters for hydrolysis of 2'dAdo-B<sub>12</sub> ( $k' = 2.58 \text{ M}^{-1} \text{ s}^{-1}$ ,  $\text{p}K_1 = 3.72$  at 90.0 °C) and those reported for 2'-deoxyadenosine ( $k' = 3.16 \text{ M}^{-1} \text{ s}^{-1}$ ,  $\text{p}K_1 = 3.60$  at 80.0 °C).<sup>34d</sup>

In light of the demonstration that above pH 4.3, 2'dAdo-B<sub>12</sub> decomposes through a combination of homolytic and heterolytic dealkylation pathways, we elected to examine the reactivity of this complex in detail. Because of the crossover in dealkylation mechanisms, the product of dealkylation of 2'dAdo-B<sub>12</sub> is expected to shift from B<sub>12r</sub>(Co<sup>II</sup>) to B<sub>12a</sub>(Co<sup>III</sup>) as the pH is lowered. Consistent with this expectation, increasing amounts of B<sub>12a</sub> were observed with decreasing pH; no B<sub>12a</sub> was observed at pH 5.28, a small amount was transiently discernible at pH 4.28, and quantitative conversion to B<sub>12a</sub> was observed at pH 3.27, see Supporting Information (Section F, p 39). However, B<sub>12a</sub> yields were generally below the expectation values, and since several competitive processes, including oxidation by trace atmospheric contamination,<sup>37</sup> self-reduction,<sup>3b,21</sup> and reduction by aldehyde<sup>3b</sup> interconvert B<sub>12r</sub> and B<sub>12a</sub>, relative B<sub>12a</sub> and B<sub>12r</sub> yields, particularly at high temperatures, are not a reliable measure of competition between homolysis and hydrolysis.

The nucleosidyl ligand products of anaerobic thermolysis of 2'dAdo-B<sub>12</sub> at 90.0 °C and pD 4.3 and 6.1 were determined by <sup>1</sup>H NMR spectroscopy (Figure 8). B<sub>12a</sub> (95% yield), adenine (47%), and *trans*-2,4-pentadienal (75%) were observed at pD 4.3 after oxidation of the decomposed sample. The pentadienal product, which results from elimination of the 3-OH from the enol tautomer of 3-hydroxy-4-pentenal,<sup>8</sup> was partially exchanged with deuterium, ca. 31%, at the H2 position. The downfield shift of the olefinic resonances reflects the  $\pi$ -conjugation in the molecule, and the large <sup>3</sup>J<sub>HH</sub> value of 15.3–15.5 Hz between H2 and H3 confirms the *trans* geometry. At pD 6.1, minor amounts of adenine and pentadienal were still produced, but the major product was an unidentified adenine derivative. Observation of a change in products from B<sub>12r</sub> and a nucleoside at high pH to B<sub>12a</sub>, adenine, and 2,4-pentadienal at lower pH is qualitatively consistent with the crossover in dealkylation

mechanisms. However, quantitative comparisons of results from kinetic and NMR product determination studies are complicated because the higher concentrations required for NMR measurements favor 2'dAdo•-B<sub>12r</sub> recombination, and hence suppress homolysis and enhance the contribution from heterolysis.

### Concluding Remarks

The studies described in this paper have demonstrated that coenzyme B<sub>12</sub> and closely related analogues thereof decompose through a variety of homolytic and heterolytic Co–C bond disruption pathways, depending on the pH, temperature, and strikingly on the substituents of the alkyl ligand. Some of the factors influencing the rates of these competing pathways and their relative contributions to the overall decomposition profile have been identified and interpreted. A striking result is the demonstration of the remarkably greater hydrolytic stability of Ado-B<sub>12</sub> compared with that of analogues lacking either the adenine or hydroxyl substituents of the 5'-deoxyadenosyl ligand. The relevance of these observations and conclusions to the biological role of coenzyme B<sub>12</sub> remains to be elucidated.

### Experimental Section

**General Methodology.** Organocobalamins were stored in the dark at 0 °C and manipulated under subdued lighting. Other air- or moisture-sensitive solids were stored in a Vacuum-Atmospheres drybox or in a vacuum desiccator. Air-sensitive reactions were performed under an atmosphere of prepurified nitrogen using standard Schlenk techniques. Anaerobic spectroscopic samples were prepared using a drybox or Schlenk line.

**Instrumentation.** <sup>1</sup>H NMR spectra were recorded on a General Electric QE-300 spectrometer and referenced to either residual organic solvent signals (CHCl<sub>3</sub> = 7.29 ppm, *d*<sub>5</sub>-DMSO = 2.49 ppm), or to 2,2,3,3-*d*<sub>4</sub>-trimethylsilylpropionate (TSP, 0.00 ppm in D<sub>2</sub>O). UV–visible spectra were recorded on a Perkin-Elmer  $\lambda$ 7 spectrophotometer equipped with a temperature-controlled cell block. pH measurements were made at room temperature relative to commercial standard buffers (pH 4.00, 7.00; Fischer) using an Orion SA520 pH meter with a combination electrode.

**Materials.** Stock and buffer solutions were prepared using distilled, deionized water. Citrate, acetate, and phosphate buffers (0.02–0.20 M) were used in the pH 1.6–3.5, 3.5–5.5, 6–8 regions, respectively. All organic solvents were reagent grade and were used without purification, except for removal of trace water by routine methods as necessary.

The following reagents were obtained from the indicated commercial sources: 5,6-dimethylbenzimidazole, 4-pentenol, adenine, dimethylglyoxime, D-ribose, benzyl chloride, pyridine-borane complex, 10% palladium on carbon, sulfur dioxide, *para*-toluenesulfonyl chloride, 2'-deoxyadenosine, adenosine, 5'-iodo-5'-deoxyadenosine, 5'-tosyladenosine, *d*<sub>4</sub>-acetic acid, and sodium *d*<sub>5</sub>-acetate were obtained from Aldrich; deuterium oxide, *d*<sub>6</sub>-dimethyl sulfoxide, and sodium 2,2,3,3-*d*<sub>4</sub>-trimethylsilyl propionate (TSP) were obtained from Cambridge Isotope Labs; vitamin B<sub>12</sub>, coenzyme B<sub>12</sub>, methyl cobalamin, 3'-deoxyadenosine, Dowex 2-X8 ion-exchange resin, and carboxymethyl cellulose were obtained from Sigma; 2',3'-dideoxyadenosine and tetrahydrofurfuryl bromide were obtained from Lancaster; 3'-deoxyadenosine also was obtained from ICN.

Literature syntheses were utilized to prepare vitamin B<sub>12r</sub>,<sup>37</sup> vitamin B<sub>12a</sub>,<sup>38</sup> 1-D-deoxyribose,<sup>39</sup> and 5'-tosyl-2'-deoxyadenosine.<sup>40</sup>

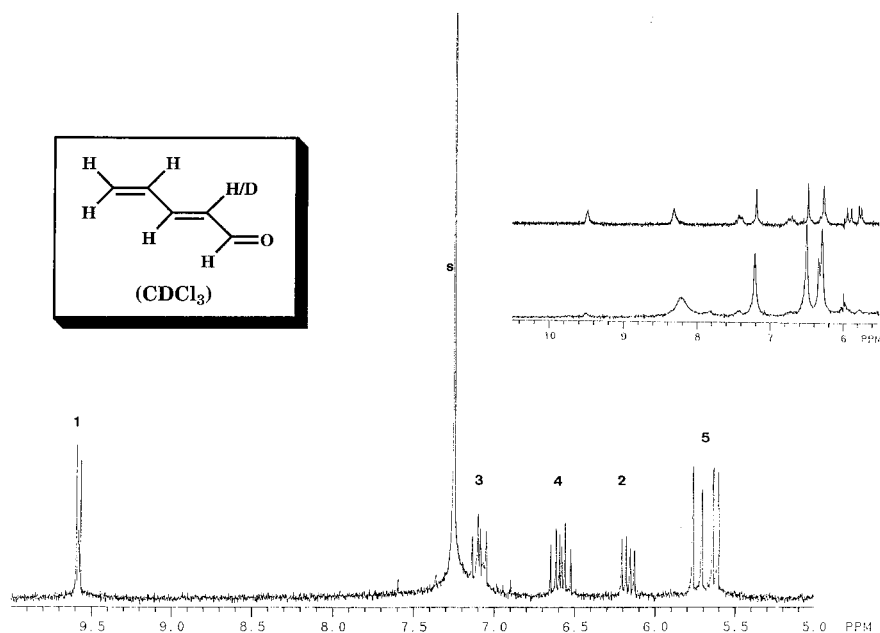
**Preparation of Organocobalt Complexes.** Requisite tosylate esters (R  $\neq$  THFF) were obtained by reaction of the corresponding nucleoside with *p*-toluenesulfonyl chloride in dry pyridine; selective reaction of the 5'-OH was confirmed by <sup>1</sup>H NMR spectra of the crude products in

(38) Bernhaur, K.; Wagner, O. *Biochem. Z.* **1963**, *337*, 366.

(39) (a) Barker, R.; Fletcher, H. G. *J. Org. Chem.* **1961**, *26*, 4605. (b) Heath, P.; Mann, J.; Walsh, E. B.; Wadsworth, A. H. *J. Chem. Soc., Perkins Trans. 1* **1983**, 2675.

(40) Robins, M. J.; McCarthy, J. R.; Robins, R. K. *Biochemistry* **1966**, *5*, 224.

(37) Blaser, H.-U.; Halpern, J. *J. Am. Chem. Soc.* **1980**, *102*, 1684.



**Figure 8.**  $^1\text{H}$  NMR spectrum of 2,4-*trans*-pentadienal, after extraction into  $\text{CDCl}_3$  from decomposed 2'dAdo- $\text{B}_{12}$  in pD 4.3 solution. Inset illustrates  $^1\text{H}$  NMR spectra recorded from the sample of 2'dAdo- $\text{B}_{12}$  decomposed anaerobically at 90.0 °C, pD 4.3 (top), and pD 6.1 (bottom).

$d_6$ -DMSO. Reliable routes to organocobalamins by reaction of nucleophilic cob(I)alamin (vitamin  $\text{B}_{12\text{s}}$ ) with tosylate esters have been described previously,<sup>41</sup> and these were employed here with modest adaptations; additional details are given in the Supporting Information (Section G, pp 40–47). Reaction of 5'-tosyladenosine with  $\text{B}_{12\text{s}}$  in methanol gave a sample with  $^1\text{H}$  NMR (Table 1)<sup>24</sup> and UV-vis<sup>41</sup> spectra identical to those recorded from a commercial sample of authentic coenzyme  $\text{B}_{12}$ .

**Axial Base Equilibrium Measurements.** Spectrophotometric acid titrations of the Ado- $\text{B}_{12}$ , 2'dAdo- $\text{B}_{12}$ , and 3'dAdo- $\text{B}_{12}$  complexes at 20.0 °C yielded equilibrium constants ( $K_1$ ) for the monoprotation (0.94–1.04 experimentally) reactions to form the base-off forms. The  $\text{p}K_1$  values differed only slightly from previous determinations, ca. 3.3 for (2'dAdo) $\text{B}_{12}$ <sup>8</sup> and 3.3–3.5 for (Ado) $\text{B}_{12}$ <sup>25</sup> vs 3.09 and 3.24 here. Temperature dependences of axial base equilibria were determined spectrophotometrically at pH 4.3 and 7.0, as described previously;<sup>21</sup> extrapolated  $\text{p}K_1$  estimates deviate  $\leq 0.6$  pH units from titration values at 20.0 °C (3.41–3.76), but errors at 90 °C should be considerably smaller because experimental accuracy increases as the equilibria shift away from base-on limits. Additional details are available in the Supporting Information (Section G, pp 40–47).

**Kinetic Measurements.** Decomposition rates were measured with modest adaptations of previously reported procedures.<sup>21</sup> Organocobalamin hydrolyses at 20.0 °C were monitored spectrophotometrically to completion ( $\geq 8t_{1/2}$ ) at 350 nm under aerobic conditions, except for the very slowest reactions ( $k_{\text{obs}} \leq 10^{-5} \text{ s}^{-1}$ ), for which endpoints were obtained by exhaustive photolysis. Reactions at 90.0 °C were monitored to completion under anaerobic conditions at the  $\text{B}_{12\text{a}}/\text{B}_{12\text{c}}$  isosbestic point near 568 nm. Additional details are given in the Supporting Information (Section G, pp 40–47).

**NMR Spectroscopy.** Dealkylation reactions were monitored by  $^1\text{H}$  NMR spectroscopy in order to identify and quantify intermediates and products. Samples of organocobalamins were dissolved in ca. 1 mL of  $\text{CD}_3\text{OD}$  and evaporated to dryness under vacuum. These were redissolved in 0.1 M  $\text{CD}_3\text{CO}_2\text{D}/\text{CD}_3\text{CO}_2^-$  or  $\text{D}_2\text{PO}_4^-/\text{DPO}_4^{2-}$  in 99.96%  $\text{D}_2\text{O}$  with 1.2 mM added TSP, to give ca. 15 mM concentrations, and were sealed in Youngs tap NMR tubes.

Decompositions were monitored periodically to completion under aerobic conditions at room temperature. Time-dependent relative

concentrations were determined by integration against the internal TSP standard. Results are shown in the Supporting Information. Olefinic products were identified by observation and distinctive H4 multiplet and H5<sub>A,B</sub> doublets between 5.0 and 6.0 ppm. H1 aldehyde signals were observed near 10.0 ppm but were often washed out by autoxidation. Characteristic spectral features of  $\text{B}_{12\text{a}}$  and adenine, where appropriate, also were observed. Hydrophobic ligand-derived organic products were isolated by extraction with  $\text{CDCl}_3$  and characterized separately.

Samples for decomposition at elevated temperatures were degassed prior to reaction by purging in a drybox. Tubes were then immersed in an oil bath. After a predetermined reaction time, tubes were cooled and opened to air and shaken in order to oxidize paramagnetic products. Spectra were then recorded and analyzed as above.

**Acknowledgment.** This research was supported in part by a grant (R37 DK13339) from the National Institutes of Health. Postdoctoral fellowship support (to M.P.J.) from the National Institutes of Health (F32 GM14924, 1/93–6/95) and the University of Chicago also is gratefully acknowledged. The editorial assistance of Joan M. Tetrault was indispensable in preparation of the manuscript.

**Supporting Information Available:** Section A, UV-visible spectra for acid titration of 3'dAdo- $\text{B}_{12}$ , titration data and fits at 20.0 °C for Ado- $\text{B}_{12}$ , 3'dAdo- $\text{B}_{12}$ , and 2'dAdo- $\text{B}_{12}$ ; Section B, temperature-dependent UV-visible spectra of 2'dAdo- $\text{B}_{12}$  at pH 7.20 and 4.28, axial base equilibrium fittings for Ado- $\text{B}_{12}$ , 3'dAdo- $\text{B}_{12}$ , and 2'dAdo- $\text{B}_{12}$ ; Section C,  $^1\text{H}$  NMR spectroscopic results for room-temperature hydrolyses of THFF- $\text{B}_{12}$  with rate data, of 1dRF- $\text{B}_{12}$ , of Ado- $\text{B}_{12}$  and 3'dAdo- $\text{B}_{12}$ , and of 2',3'ddAdo- $\text{B}_{12}$  and 2'dAdo- $\text{B}_{12}$  with rate data; Section D, UV-visible spectral changes during hydrolysis of THFF- $\text{B}_{12}$  at pH 3.31 and 20 °C, pH-dependent rate data and fits for all six complexes at 20 °C; Section E, pH-dependent kinetic rates and fits at 90 °C for Ado- $\text{B}_{12}$ , 3'dAdo- $\text{B}_{12}$ , 2'dAdo- $\text{B}_{12}$ ; Section F,  $\text{B}_{12\text{c}}$  rate suppression data for 2'dAdo- $\text{B}_{12}$  at pH 4.28 and 90 °C and pH-dependent spectral changes for 2'dAdo- $\text{B}_{12}$  dealkylation at 90 °C; Section G, experimental details (PDF). This material is available free of charge via the Internet at <http://pubs.acs.org>.

(41) (a) Smith, E. L.; Mervyn, L.; Johnson, A. W.; Shaw, N. *Nature* **1962**, *194*, 1175. (b) Muller, O.; Muller, G. *Biochem. Z.* **1962**, *336*, 299. (c) Johnson, A. W.; Mervyn, L.; Shaw, N.; Smith, E. L. *J. Chem. Soc.* **1963**, 4146. (d) Dolphin, D. *Methods Enzymol.* **1971**, *18C*, 34. (e) Hogenkamp, H. P. C. *Biochemistry* **1974**, *13*, 2736.